Challenges in Object Detection Under Rainy Weather Conditions

Sinan Hasirlioglu[1,2(✉)] and Andreas Riener[1,2]

[1] Technische Hochschule Ingolstadt, CARISSMA, 85049 Ingolstadt, Germany
Sinan.Hasirlioglu@carissma.eu
[2] Johannes Kepler University Linz, 4040 Linz, Austria
http://www.carissma.eu

Abstract. Intelligent vehicles use surround sensors which perceive their environment and therefore enable automatic vehicle control. As already small errors in sensor data measurement and interpretation could lead to severe accidents, future object detection algorithms must function safely and reliably. However, adverse weather conditions, illustrated here using the example of rain, attenuate the sensor signals and thus limit sensor performance. The indoor rain simulation facility at CARISSMA enables reproducible measurements of predefined scenarios under varying conditions of rain. This simulator is used to systematically investigate the effects of rain on camera, lidar, and radar sensor data. This paper aims at (1) comparing the performance of simple object detection algorithms under clear weather conditions, (2) visualizing/discussing the direct negative effects of the same algorithms under adverse weather conditions, and (3) summarizing the identified challenges and pointing out future work.

Keywords: Object detection · Camera · Lidar · Radar · Perception · Rain · Adverse weather condition · Vehicle safety · Autonomous driving

1 Introduction

Active and integral safety systems rely on data given by surround sensors such as camera, lidar, and radar. Using the obtained information, control systems can take over forward and sideways guidance of vehicles in order to assist the driving task or to prevent imminent accidents. These systems could thus be regarded as precursors on the way to autonomous driving. However, each surround sensor has limited capabilities under certain circumstances, especially under adverse weather conditions [11,12]. Water droplets in the air cause scattering and absorption effects and limit sensor performance. Note that incorrect detections and classifications increase the risk of an accident.

Each sensor type outputs raw data with different physical unit and quantity. In this work, we focus on images of camera sensors, point clouds of lidar sensors,

J. C. Ferreira et al. (Eds.): INTSYS 2018, LNICST 267, pp. 53–65, 2019.
https://doi.org/10.1007/978-3-030-14757-0_5

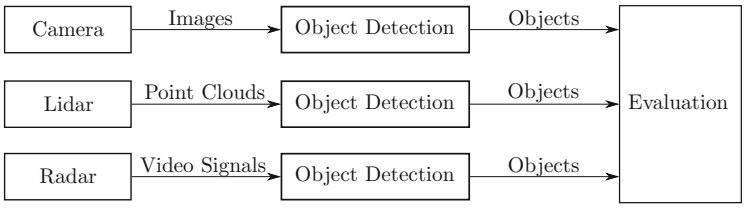

Fig. 1. Procedure for investigating the weather effects on object detection algorithms. Each surround sensor type is analyzed individually.

and video signals of radar sensors. Figure 1 shows the general procedure for investigating weather effects on object level. The effects are sensor specific and must be investigated individually.

Object detection algorithms process raw sensor data to detect objects in the surrounding. The camera algorithms used in this work output bounding boxes with corresponding classification scores. In case of lidar, the algorithms group points into ground plane and obstacles. Lastly, the radar algorithms detect objects when the received intensity exceeds an adaptive threshold value.

Outline

This paper aims to present challenges under rainy conditions. Object detection algorithms that process data from two identical scenarios with various weather conditions are investigated. Even minor changes in sensor data can lead to major challenges in the detection task. Therefore, testing algorithms under adverse weather conditions is mandatory to ensure safe autonomous driving.

This paper is organized as follows. Section 2 gives an overview on related work done in the field of object detection under adverse weather conditions. Further, Sect. 3 describes the experimental setup and used object detection algorithms for each sensor type. Section 4 discusses the results and challenges under rainy conditions where Sect. 5 presents the scientific contribution of this paper.

2 Related Work

In this section, we will present the related work with focus on object detection under adverse weather conditions. Today, the robustness is mainly tested in clear weather conditions, while only little research is focusing on adverse conditions.

2.1 Camera

Garg and Nayar published several works about the effects of rain on camera. In [5], a geometric and photometric model for refraction and reflection from a single raindrop was presented. It was shown that raindrops redirect light from a large field of view (approx. 165°). Therefore, the brightness of raindrops does not depend absolutely on their background. However, falling drops result in rain streaks which depend on their background and the exposure time of the camera

[6]. A method in order to reduce the effects of rain by setting the camera parameters (exposure time, F-number, distance of the focal plane) was presented in [7]. More practical work was presented by Duthon et al. [2] in which they generated artificial rain in the laboratory and investigated the impact of rain by using the Harris Corner Detector. The authors showed that lower rain intensities (approx. 40 mm/h) has nearly no influence on the Harris feature, whereas higher intensities (approx. 130 mm/h) strongly impact the feature. The authors in [12] showed that raindrops lead to increasing mean intensity of the image and decreasing contrast, where the rain conditions are also generated by a rain simulator.

This work focuses on the influence of rain on object detection, in which we investigate the detection (based on histogram of oriented gradients (HOG) features) and classification (based on AlexNet) separately.

2.2 Lidar

Wojtanowski et al. [19] showed that the impact of atmospheric extinction on lidar is much more crucial than the impact of surface wetness. The light propagating through the medium of rain gets strongly attenuated which drastically decreases the sensor performance. Rasshofer et al. [15] showed that water drop reflections could result in false positive scan points, especially in the near field (<10 m). By using an indoor rain simulator, they investigated the maximum detection range with different target reflectivities, sensors, and rain intensities. The higher the rain intensity and the lower the target reflectivity, the shorter the detection range. The authors in [12] showed that in case of high rain intensity the false positives dominate which may hide the object completely. Using the multi echo technology, object points can still be detected but with drastically decreased intensity. Note that the sensor behavior is strongly hardware-dependent, due to the fact that internal signal processing is unknown.

This paper focuses on the influence of rain on the clustering process of standard algorithms and presents additional challenging secondary effects.

2.3 Radar

The influence of rain on automotive radar sensors have been studied in [13], where a reduction of the millimeter-wave signal can be observed. An electromagnetic wave traveling through rain will be absorbed, depolarized, scattered, and delayed in time. Unlike lidar sensor, strong performance degradation can be detected when a water film covers the radome. Gourova et al. [8] presented experimental data of a standard automotive radar sensor and demonstrated the detectability of strong rain, generated with a rain simulator. They conclude that raindrops are especially visible in the near field (2–3 m). The authors in [12] showed that the radar cross section values of surrounding objects decrease in rainy scenarios and can lead to incorrect classification.

In this work, we focus on the influence of rain on adaptive threshold algorithms, that are used for detecting objects based on the received intensity.

3 Materials and Methods

In this section, we present the experimental setup used for gathering data from surround sensors and the object detection algorithms.

3.1 Experimental Setup

Measurements are performed in the CARISSMA test facility which is equipped with an indoor rain simulator capable of simulating various intensities and drop size distributions over a length of 50 m. Rain is generated by different full cone nozzle combinations. For this work, a rain intensity of 100 mm/h is selected to make the effects clearly visible.

The sensor setup is placed in front of the rain simulator due to the fact that not all sensors are waterproof. The images are recorded by an uEye camera (U3-3250LE-C-HQ) with a resolution of 1.92 MP and a 6 mm focal length lens. Lidar measurements are performed using a Velodyne VLP-16 sensor, which outputs a point cloud with 16 layers. The video signals are output of the Inras RDL-77G-TX2RX16 radar. We set the sweep bandwidth to 300 MHz and the ramp slope to 10 MHz/µs, which results in a range resolution of 0.5 m. The measurements are performed with and without rain. For reproducible results, we use a standardized Euro NCAP Vehicle Target (EVT) [16] which is placed at a distance of 10 m from the sensors without a lateral offset. This setup is imitating an urban car-following scenario. Figure 2 shows the test area in both conditions without a target. Further, it is assumed that the rain is distributed uniformly in the sensor's field of view.

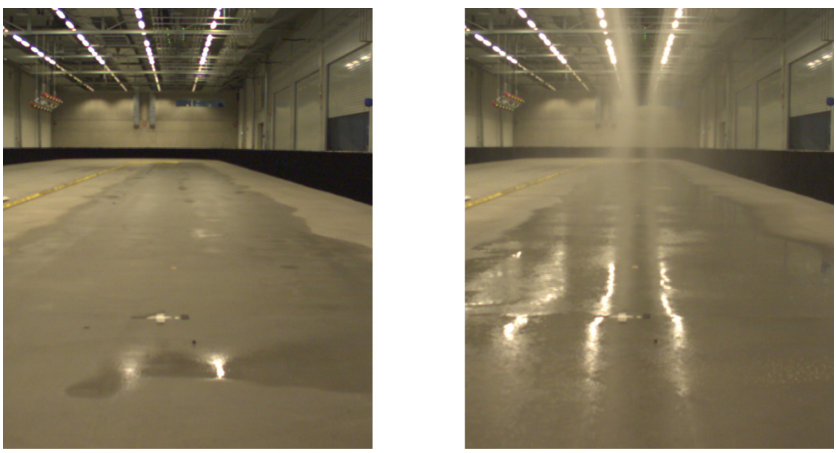

Fig. 2. CARISSMA test facility with an indoor rain simulator that enables measurements from identical scenarios with various weather conditions. The full cone nozzles produce many small water drops which lead to decreased visibility. It is assumed that the rain is distributed uniformly in the sensor's field of view.

3.2 Object Detection Based on Camera

In this work, objects are detected in images by combining a cascade object detector [18] based on HOG features [1] with a pre-trained AlexNet model [14]. The cascade object detector provides the bounding box which defines the region of interest (ROI) for the classification based on AlexNet. Figure 3 shows the result of object detection and classification under clear conditions. The camera output is cropped to the size of 640×480 pixels.

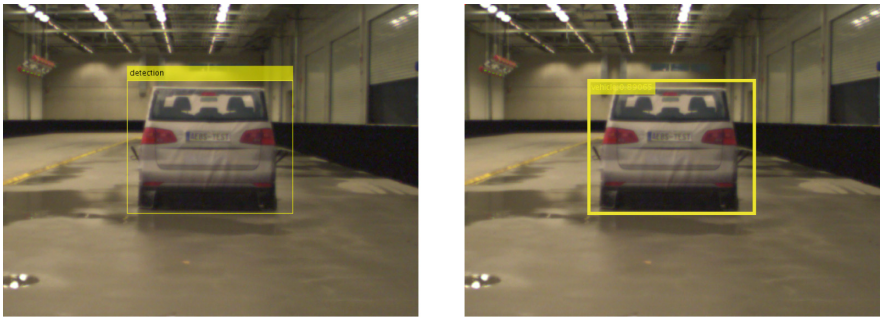

Fig. 3. Detection using a cascade object detector based on HOG (left) and classification based on AlexNet model (right), which results in a score of 0.89.

Cascade object detection is a machine learning approach, in which a HOG-based object detector is trained by a set of positive and negative images. In this work, we provided 233 positive images of rear views of different vehicles and 380 negative images without vehicles. Training the cascade detector is applied in form of simple stages where each stage is considered to be a weak learner. Each stage is trained by using all provided positive samples and a part of the negative image set. More negative samples are automatically generated from detections in the provided negative images. In this way, each new stage will be trained to correct mistakes done by previous stages, which results in a robust detector at the end. We defined 50 stages and 50% false positive rate to achieve our results.

For classification, a transfer learning on AlexNet neural network is implemented, which is an approach to reuse a pre-trained model or network and customize it for another task. The pre-trained AlexNet model has been trained on more than a million images and can classify 1000 object categories [14]. Relevant objects in traffic scenarios are obstacles such as vehicles, pedestrians, or traffic signs. Via transfer learning, the newly created model will classify only these relevant objects. The final three layers of the model use features extracted from the initial layers for classification. Therefore, only weight values of the final layers are tuned, whereas those of the initial layers are constant.

3.3 Object Detection Based on Lidar

Lidar sensors provide position and signal strength (intensity) information of each single scan point of the point cloud. In this paper, we focus on two basic algorithms that process position information. The ground plane segmentation is based on a variant of the random sample consensus (RANSAC) [4,17], whereas the clustering is based on a density-based algorithm.

The ground plane detection algorithm groups data into inliers and outliers where the former one is determined by a chosen model. Here, we used the z-plane as model input to determine the ground plane and subtract it from the original point cloud. Therefore, a new point cloud is generated containing only obstacle scan points. Note that the segmentation process in complex real world scenarios is more challenging due to up and down gradients of the roads.

Clustering of lidar scan points into objects or obstacles is performed using the density-based spatial clustering of applications with noise (DBSCAN) algorithm [3], which groups points that are close to each other based on a distance measure (e.g., Euclidean distance) and minimum number of points. The algorithm marks points, which are not in dense regions as outliers. Figure 4 shows the results under clear weather conditions.

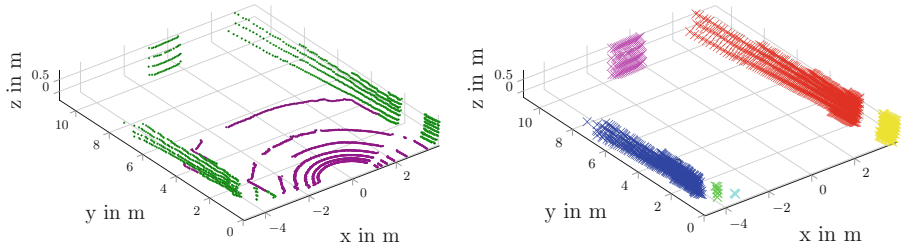

Fig. 4. Point cloud after ground plane segmentation (left) and clustering (right). The multi-layer lidar sensor detects the target vehicle with four layers, which are clustered correctly and highlighted in pink. (Color figure online)

The left image shows the segmented point cloud, where the magenta points belong to the ground plane and the green points to objects and obstacles in the surrounding. The image on the right side shows the results of the clustering process, where all green points from the left image are divided into groups and marked with different colors. It can be seen that the algorithms perform well under clear weather conditions. All ground reflections are detected and separated from the initial point cloud. The target object is clustered clearly and highlighted in pink. The remaining clusters originate from the barriers (see Fig. 2).

3.4 Object Detection Based on Radar

This work focuses on object detection based on reflected intensity from surrounding objects. In addition to direct target reflections, the sensor receives reflections

from unwanted objects (also called clutter). Adaptive threshold algorithms based on different constant false alarm rate (CFAR) techniques are implemented for filtering unwanted signals and detecting objects of interest. We focus on cell averaging (CA-CFAR), cell averaging smallest of (CASO-CFAR), cell averaging greatest of (CAGO-CFAR), and order statistic (OS-CFAR) methods.

In CFAR systems, target decisions are performed using the sliding window technique, where the data of a reference window enter an algorithm for calculating the decision threshold T based on clutter power Z and scaling factor S. For estimating Z, the sliding window is split into leading and lagging part. CA-CFAR uses the average of the averaged two parts as the clutter power Z. CASO-CFAR and CAGO-CFAR combine the neighboring parts by selecting the minimum (CASO) or the maximum (CAGO). The OS-CFAR method sorts all cells inside the sliding window in ascending order and selects one certain value as Z. A more detailed overview is given in [9] and [10]. The results based on the radar output can be seen in Fig. 5.

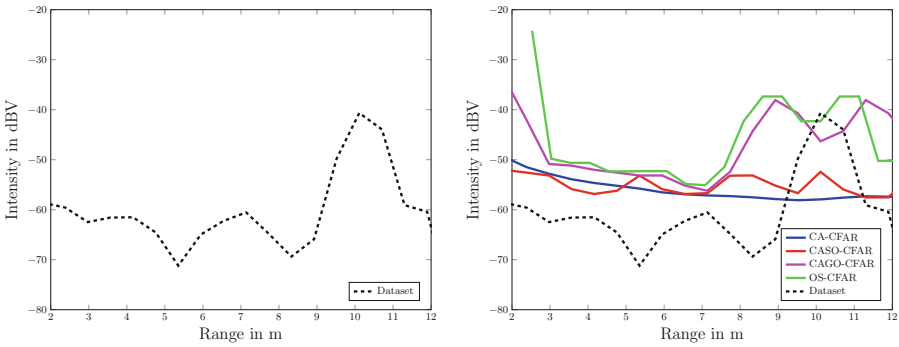

Fig. 5. Video signal under clear conditions, in which the target is positioned at a distance of 10 m (left) and the corresponding CFAR thresholds (right).

The left image shows the video signal in clear weather conditions. It can be seen that the target object at a distance of 10 m causes the highest reflections. The remaining reflections are considered as clutter. The image on the right side shows the result of the object detection based on CFAR algorithms. The sliding window size is chosen as $N = 6$ and the scaling factor as 0.85. For OS-CFAR, the reference cell value is chosen as 5th maximum. All CFAR techniques can detect the target vehicle. Note that a lower threshold can lead to closer object position.

4 Experimental Results and Discussion

In this section, we present the influences of rain on object detection algorithms, introduced in the previous section, and discuss potential challenges.

4.1 Camera

The results of the object detection can be seen in Fig. 6. The left image shows the detection without rain with a classification score of 0.89. The image on the right shows the detection with rain, where the score is decreased by 21%. Further, it can be seen that the bounding box is shifted to the left by 13 pixels and increased in size by 6%. Note that incorrect position or size estimations can lead to incorrect crash severity predictions. If the target is placed at a distance of 30 m, the algorithms detect exclusively false positives for both conditions, as they are classified by the AlexNet model as background. Hence, raindrops have a direct negative influence on image features and therefore on the object detection task.

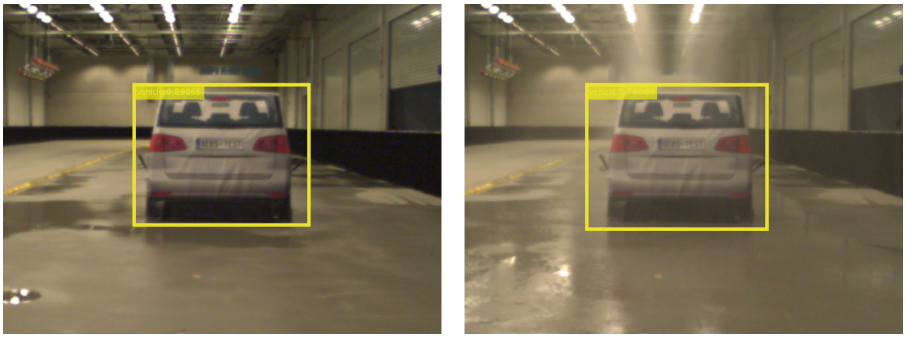

Fig. 6. Object detection without rain (left) and with rain (right). The score decreases from 0.89 to 0.70. The bounding box is shifted to the left by 13 pixels and covers a 6% larger region.

For a more in-depth analysis, we visualize the distribution of oriented gradients under both weather conditions. It is known, that rain decreases the image contrast and creates blurry effects. Figure 7 shows the histograms of the gray scaled images of the target vehicle without (left) and with (right) rain. The ROI is limited to the vehicle region. The channels spread over 0 to 180° using nine bins. It can be seen that the gradient magnitudes decrease drastically and result in a new histogram shape. The total magnitude (sum of all bins) decreases under rainy conditions by 49%, which originates from smaller intensity changes around edges and corners. It can therefore be concluded that rainy conditions affect raw sensor data and limit the general sensor performance.

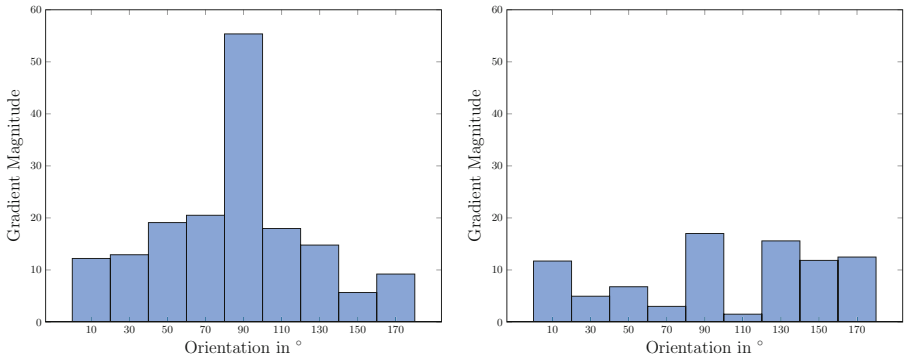

Fig. 7. Comparison of HOG histograms in clear (left) and rainy (right) conditions. The bins represent nine orientation angles. The total magnitude decreases in rainy conditions by 49%.

4.2 Lidar

Rainy conditions are directly related to falling water drops and wet ground. The left image in Fig. 8 shows the direct influence of rain on the lidar measurement. The number of target vehicle scan points decreases by only 4%. However, some transmitted light beams are deflected by the wet ground plane and form a mirror image of the target vehicle below the ground. Therefore, an object at a distance of 10 m is detected with 8 layers. This effect also occurs in images of camera sensors in a weakened form (see image on the right of Fig. 6). Note that false positive scan points, due to ground reflections, lead to missing ground plane points. False positive scan points can also originate from falling drop reflections, which are mainly visible in the near field.

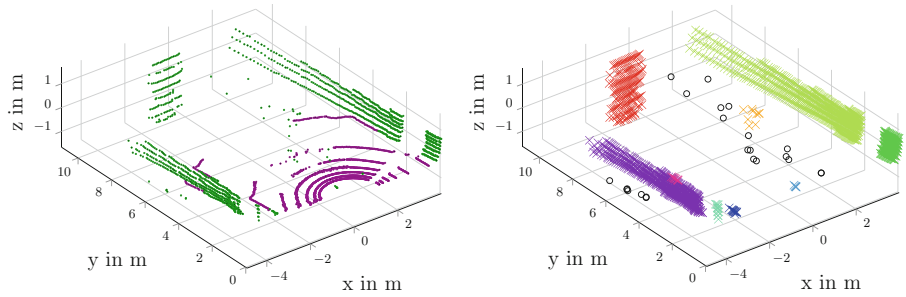

Fig. 8. Point cloud under rainy conditions including ground plane segmentation (left) and clustering (right). Raindrop reflections can lead to false positive clusters, whereby ground reflections can form a mirror image of the target vehicle. (Color figure online)

The image on the right side of Fig. 8 shows the result of clustering in rainy conditions. The ground reflections cause a mirror image whose scan points are close to the real target reflections. Therefore, the algorithm clusters these points to one object which is highlighted in red. The size is increased to about twice. Moreover, falling drop reflections can also be close to each other and result in clusters. Two false positive objects can be detected between sensor and target vehicle. The majority of the raindrops reflections are detected as noise.

Further, rainy conditions affect the intensity of scan points. Absorption and scattering processes reduce the amount of power, which is backscattered to the receiver. Figure 9 illustrates different histograms under clear and adverse weather conditions to show the influence in detail. Note that the intensity value depends on the incident angle. A small angle to the vertical means that the intensity value is likely to be higher in comparison to a large angle.

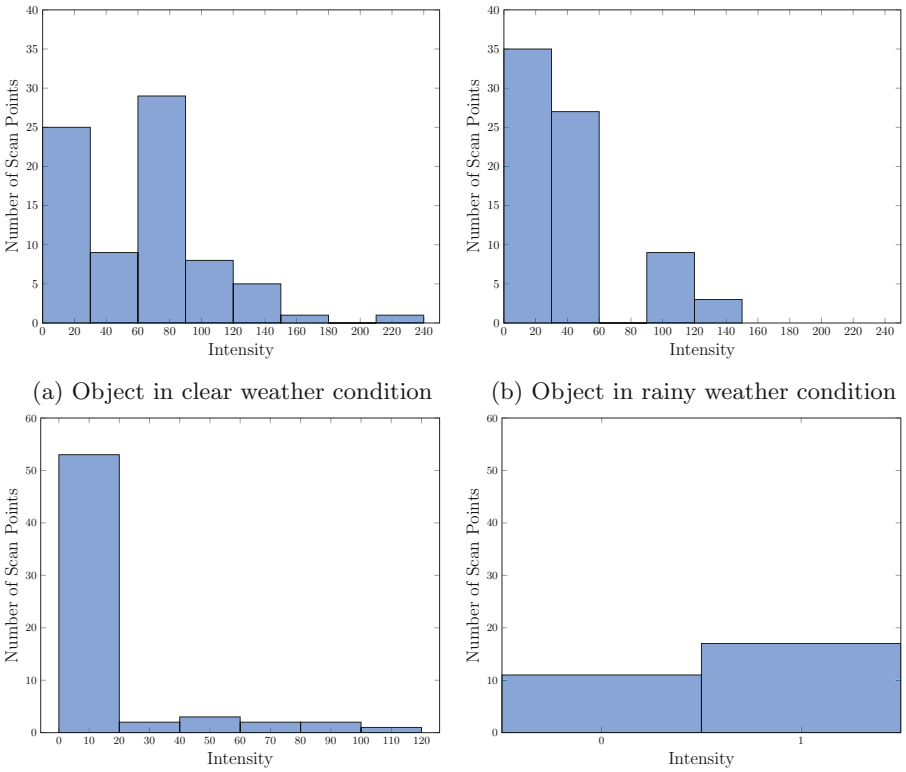

(a) Object in clear weather condition

(b) Object in rainy weather condition

(c) Mirror image of target object

(d) Raindrop reflections

Fig. 9. Intensity histograms of specific point clouds. The intensity of target object reflections in clear weather condition is represented in (a). Rain leads to decreasing object intensity (b), low intensity mirror image below the ground (c), and low intensity raindrop reflections (d).

The intensity histogram of the target vehicle under clear conditions shows a wide range due to varying incident angles (see Fig. 9(a)). In case of rain, the intensities decrease and the bars are shifted to the left (Fig. 9(b)). The resulting mirror image contains mainly scan points with low intensities, but also some points with higher intensities (see Fig. 9(c)). The falling water drop reflections are limited to values between 0 and 1 (Fig. 9(d)). Therefore, a simple intensity-based filtering is associated with loosing true positive scan points. It can be concluded that rain leads to challenging segmentation and clustering tasks.

4.3 Radar

Raindrops scatter the transmitted wave back to the sensor which is visible in the measured video signal. Figure 10 shows the received signal and adaptive thresholds under clear and adverse weather conditions.

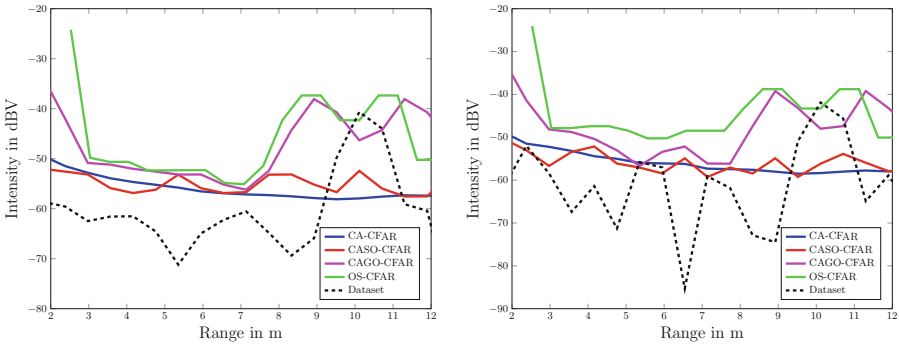

Fig. 10. Video signal (black dotted line) and different CFAR threshold values under clear (left) and rainy (right) conditions.

The left image shows the measured video signal (black dotted line) and the performance of different CFAR algorithms in clear conditions, where the image on the right shows the performance in rainy conditions. It can be seen that the video signal in rainy conditions has higher intensity in the near field which decreases with distance. The object reflection decreases by 1.23 dB due to extinction caused by water particles, but can be neglected in this work.

In clear conditions, all algorithms can detect the target object at 10 m precisely. The increased near field reflections under rain lead to changes in threshold values. CASO-CFAR detects a false positive object at a distance of approx. 2.5 m. At a distance of approx. 5 m CASO-CFAR, CAGO-CFAR, and CA-CFAR output incorrect detections. Further, CASO-CFAR detects two more false positive objects at distances of approx. 6 and 7 m. The target object is visible for each algorithm. The OS-CFAR performs best without any false detections. Hence, it can be concluded that adaptive threshold algorithms have possibilities of false detections in non-homogeneous environment (with more clutter peaks).

5 Conclusion

Intelligent safety systems are reliant on data from surround sensors such as camera, lidar, and radar. Using this information, control systems can take over the forward and sideways guidance of vehicles in order to assist the driver or to prevent imminent accidents. It is known that sensor signals suffer much attenuation while propagating through the atmosphere, especially under adverse weather conditions. This paper presents the influence of rain on basic object detection algorithms for camera, lidar, and radar sensors. Initial static tests show that each sensor can generate false positive objects due to changed weather condition. The problem is that incorrect environmental perception, especially in the area of integral safety, can result in incorrect actions and hence severe accidents.

Camera sensors suffer mainly from decreased gradient magnitudes, which result in changed position and size of the bounding boxes during the detection task. Further, the classification scores can decrease which represent the increasing uncertainty. Lidar sensors can generate false positive scan points or even false positive objects from raindrop reflections. Moreover, the wet ground can lead to deflections of the laser light which can result in mirror images below the ground. These effects increase the complexity of ground plane detection and scan point clustering. Radar sensors receive the backscattered waves from raindrops which lead to increased reflection intensities in the near field. Scattering and absorption processes result in decreased object intensity, which can be neglected within close distances. Changes in received intensity are associated with changes in threshold values, so that three of four algorithms under test generate false positive objects.

Future work includes the use of additional detection algorithms for all types of surround sensors. Furthermore, different objects enable the investigation of false classifications in detail. More in-depth analysis is intended by varying the rain intensity from low to extremely high. Finally, dynamic tests can increase the level of realism and include the benchmark of tracking algorithms.

Acknowledgment. We applied the SDC approach for the sequence of authors. The authors would like to thank the master students Al-Bahr Ayad Ameen Sadeq, Altinbas Selim, Intriz Ercan, Ladva Ronak Madhavji, Malaviya Ujval Jaysukhbhai, and Nguyen Huu Anh Huy for implementing the detection algorithms and analyzing the influences on object-level. This work is supported under the FH-Impuls program of the German Federal Ministry of Education and Research (BMBF) under Grant No. 13FH7I01IA.

References

1. Dalal, N., Triggs, B.: Histograms of oriented gradients for human detection. In: 2005 IEEE Computer Society Conference on Computer Vision and Pattern Recognition (CVPR 2005), pp. 886–893. IEEE (2005)
2. Duthon, P., Bernardin, F., Chausse, F., Colomb, M.: Methodology used to evaluate computer vision algorithms in adverse weather conditions. Transp. Res. Procedia **14**, 2178–2187 (2016)

3. Ester, M., Kriegel, H.P., Sander, J., Xu, X.: A density-based algorithm for discovering clusters a density-based algorithm for discovering clusters in large spatial databases with noise. In: Proceedings of the Second International Conference on Knowledge Discovery and Data Mining, KDD 1996, pp. 226–231. AAAI Press (1996)
4. Fischler, M.A., Bolles, R.C.: Random sample consensus: a paradigm for model fitting with applications to image analysis and automated cartography, vol. 24, pp. 381–395. ACM, New York (1981)
5. Garg, K., Nayar, S.K.: Photometric model of a rain drop. CMU Technical report (2003)
6. Garg, K., Nayar, S.K.: Detection and removal of rain from videos. In: Computer Vision and Pattern Recognition (2004)
7. Garg, K., Nayar, S.K.: Vision and rain. Int. J. Comput. Vis. **75**(1), 3–27 (2007)
8. Gourova, R., Krasnov, O., Yarovoy, A.: Analysis of rain clutter detections in commercial 77 GHz automotive radar. In: 2017 European Radar Conference EURAD, pp. 25–28 (2017)
9. Rohling, H.: Radar CFAR thresholding in clutter and multiple target situations. IEEE Trans. Aerosp. Electron. Syst. **AES–19**(4), 608–621 (1983)
10. Rohling, H.: Ordered statistic CFAR technique - an overview. In: 2011 12th International Radar Symposium (IRS), pp. 631–638 (2011)
11. Hasirlioglu, S., Doric, I., Kamann, A., Riener, A.: Reproducible fog simulation for testing automotive surround sensors. In: 2017 IEEE 85th Vehicular Technology Conference (VTC Spring), pp. 1–7. IEEE (2017)
12. Hasirlioglu, S., Kamann, A., Doric, I., Brandmeier, T.: Test methodology for rain influence on automotive surround sensors. In: 2016 IEEE 19th International Conference on Intelligent Transportation Systems (ITSC), pp. 2242–2247. IEEE (2016)
13. Hassen, A.A.: Indicators for the signal degradation and optimization of automotive radar sensors under adverse weather conditions: Zugl.: Darmstadt, Techn. Univ., Diss., 2006. Berichte aus der Hochfrequenztechnik, Shaker, Aachen (2007)
14. Krizhevsky, A., Sutskever, I., Hinton, G.E.: ImageNet classification with deep convolutional neural networks. In: Proceedings of the 25th International Conference on Neural Information Processing Systems - Volume 1, NIPS 2012. pp. 1097–1105. Curran Associates Inc., USA (2012)
15. Rasshofer, R.H., Spies, M., Spies, H.: Influences of weather phenomena on automotive laser radar systems. Adv. Radio Sci. **9**, 49–60 (2011)
16. Sandner, V.: Development of a test target for AEB systems. In: 23rd International Technical Conference on the Enhanced Safety of Vehicles (ESV): Research Collaboration to Benefit Safety of All Road Users (2013)
17. Torr, P., Zisserman, A.: MLESAC: a new robust estimator with application to estimating image geometry. Comput. Vis. Image Underst. **78**(1), 138–156 (2000)
18. Viola, P., Jones, M.: Rapid object detection using a boosted cascade of simple features. In: Proceedings of the 2001 IEEE Computer Society Conference on Computer Vision and Pattern Recognition, CVPR 2001. pp. I-511–I-518. IEEE (2001)
19. Wojtanowski, J., Zygmunt, M., Kaszczuk, M., Mierczyk, Z., Muzal, M.: Comparison of 905 nm and 1550 nm semiconductor laser rangefinders' performance deterioration due to adverse environmental conditions. Opto-Electron. Rev. **22**(3), 183–190 (2014)